Diagn Interv Radiol 2023; DOI: 10.4274/dir.2023.232284

ABDOMINAL IMAGING

ORIGINAL ARTICLE

Prostate zones and tumor morphological parameters on magnetic resonance imaging for predicting the tumor-stage diagnosis of prostate cancer

Shanshan Xu
Xiaobing Liu
Xiaoqin Zhang
Huihui Ji
Runyuan Wang
Huilin Cui
Jinfeng Ma
Yongjian Nian
Yi Wu
Ximei Cao

PURPOSE

To determine whether the morphological parameters of prostate zones and tumors on magnetic resonance imaging (MRI) can predict the tumor-stage (T-stage) of prostate cancer (PCa) and establish an optimal T-stage diagnosis protocol based on three-dimensional reconstruction and quantization after image segmentation.

METHODS

A dataset of the prostate MRI scans and clinical data of 175 patients who underwent biopsy and had pathologically proven PCa from January 2018 to November 2020 was retrospectively analyzed. The authors manually segmented and measured the volume, major axis, and cross-sectional area of the peripheral zone (PZ), transition zone, central zone (CZ), anterior fibromuscular stroma, and tumor. The differences were evaluated by the One-Way analysis of variance, Pearson's chi-squared test, or independent samples *t*-test. Spearman's correlation coefficient and receiver operating characteristic curve analyses were also performed. The cut-off values of the T-stage diagnosis were generated using Youden's J index.

RESULTS

The prostate volume (PV), PZ volume (PZV), CZ volume, tumor's major axis (TA), tumor volume (TV), and volume ratio of the TV and PV were significantly different among stages T1 to T4. The cut-off values of the PV, PZV, CZV, TA, TV, and the ratio of TV/PV for the discrimination of the T1 and T2 stages were 53.63 cm^3, 11.60 cm^3, 1.97 cm^3, 2.30 mm, 0.90 cm^3, and 0.03 [area under the curves (AUCs): 0.628, 0.658, 0.610, 0.689, 0.724, and 0.764], respectively. The cut-off values of the TA, TV, and the ratio of TV/PV for the discrimination of the T2 and T3 stages were 2.80 mm, 8.29 cm^3, and 0.12 (AUCs: 0.769, 0.702, and 0.688), respectively. The cut-off values of the TA, TV, and the ratio of TV/PV for the discrimination of the T3 and T4 stages were 4.17 mm, 18.71 cm^3, and 0.22 (AUCs: 0.674, 0.709, and 0.729), respectively.

CONCLUSION

The morphological parameters of the prostate zones and tumors on the MRIs are simple and valuable diagnostic factors for predicting the T-stage of patients with PCa, which can help make accurate diagnoses and lateral treatment decisions.

KEYWORDS

Magnetic resonance imaging, prostate neoplasms, prostate zones, tumor volume, neoplasm-stage

From the Department of Digital Medicine (S.X., X.L., X.Z., R.W., Y.N., Y.W. ✉wuy1979@tmmu.edu.cn), College of Biomedical Engineering and Medical Imaging, Army Medical University (Third Military Medical University), Chongqing, China; Department of Histology and Embryology (S.X., H.J., R.W., H.C., X.C. ✉caoximei@163.com), Shanxi Medical University, Taiyuan, China; Department of Urology (X.L.), Xinqiao Hospital of Army Medical University, Chongqing, China; Department of General Surgery (J.M.), Shanxi Province Cancer Hospital of Shanxi Medical University, Taiyuan, China, Yu-Yue Pathology Research Center, Jinfeng Laboratory (S.X., Y.W.) Chongqing 401329, People's Republic China.

Received 27 April 2023; revision requested 30 May 2023; last revision received 11 August 2023; accepted 23 August 2023.

Epub: 03.10.2023

Publication date: 07.11.2023

DOI: 10.4274/dir.2023.232284

Prostate cancer (PCa) is the second most frequent cancer with the fifth highest mortality rate worldwide.[1] The prostate is an anatomically heterogeneous organ, mainly including the peripheral zone (PZ), transition zone (TZ), central zone (CZ), and anterior fibromuscular stroma (AFMS).[2] On pathological biopsies, PCa is often a multifocal cancer with histologic heterogeneity of different tumor foci, with most tumors in the PZ. As the disease progresses, the tumor invades the adjacent zones and the surrounding fat, seminal vesicles (SV), bladder, and rectum, causing distant metastasis. Thus, PCa can rapidly progress from local inertia to fatal metastatic disease. Furthermore, as the aging population has increased, the incidence of

You may cite this article as: Xu S, Liu X, Zhang X, et al. Prostate zones and tumor morphological parameters on magnetic resonance imaging for predicting the tumor-stage diagnosis of prostate cancer. *Diagn Interv Radiol.* 2023;29(6):753-760.

PCa has also considerably increased, posing an important diagnostic challenge.

Traditionally, patients with suspected PCa after a digital rectal examination (DRE) or prostate-specific antigen (PSA) test require a trans-rectal ultrasound (TRUS)-guided systematic biopsy, which is the current gold standard for diagnosing PCa.[3] However, magnetic resonance imaging (MRI) examinations have become the preferred option since they reduce the number of biopsies carried out and allow more patients to be enrolled in active surveillance programs. There are also many benefits of using MRI for diagnosis. First, unlike DRE and TRUS, MRI is non-invasive.[4] Second, MRI displays the anatomical regions of the prostate better than computed tomography exams. Third, MRI is the gold standard for delineating tumor volume (TV) in PCa, which directly contributes to the tumor-node-metastasis stage (TNM) diagnosis; the TNM stage is critical for selecting the treatment strategy, improving the prognosis, and avoiding or reducing side effects.[5] Fourth, the prostate volume (PV) calculated from a three-dimensional (3D) reconstruction model based on slide-by-slide, manually segmented MRIs is more accurate than the PV calculated from the commonly used ellipsoid formula based on ultrasound images.[6]

Accurately measuring the morphological parameters of the prostate zones and the tumor is necessary for diagnosing and treating PCa.[7-9] For example, the PV helps to determine the appropriate radiotherapy, and the TV has been associated with clinical manifestations of PCa. In addition, some studies have reported the relationship between some morphological parameters (PZ volume, TZ volume, and PV) and benign prostatic hyperplasia (BPH) and PCa. However, few anatomical or pathological studies on the four prostate zones (PZ, TZ, CZ, and AFMS) exist.[10-12] However, to the best of the authors' knowledge, there is little research on the morphological parameters and tumor-stage (T-stage) diagnosis of PCa in the literature that the authors have retrieved.

Main points

- A positive correlation exists between the tumor-stage (T-stage) and quantitative morphological parameters of prostate cancer (PCa).
- The tumor's major axis, tumor volume, and volume ratio of the tumor and prostate can be used as important factors to diagnose the T-stage of PCa.
- The quantitative morphological parameters of the tumor are valuable in improving prognostic and lateral treatment decisions.

Herein, the authors investigated the diagnostic roles of the morphological parameters of the prostate zones and prostate tumor on the PCa T-stage to assist clinicians with T-stage diagnoses, prognostic judgments, and the surgical selection of patients with PCa.

Methods

Study population and data acquisition

Patients

This retrospective study was approved by the Medical Ethics Committee of Shanxi Cancer Hospital (2021051) and The Second Affiliated Hospital of Army Medical University, PLA (2022-YD 460-01). The informed consent requirement was waived since these MRI scans were acquired during routine clinical care.[8]

For this study, the authors obtained the detailed medical histories of 221 patients with PCa treated at the Shanxi Cancer Hospital (n = 42) and The Second Affiliated Hospital of Army Medical University (n = 179) from January 2018 to November 2020. The inclusion criteria were (1) patients who had had an MRI scan due to an increase of PSA and/or the suspicion of PCa by DRE and (2) had undergone multiparametric MRI (mp-MRI) with subsequent 12-core TRUS–guided biopsy and an MRI/TRUS fusion biopsy. The exclusion criteria were patients (1) with a history of (a) endocrine therapy (n = 13), (b) laparoscopic radical prostatectomy (n = 10), and/or (c) transurethral resection (n = 16), and / or (2) who had substandard image quality where the PZ, TZ, CZ, and AFMS were unidentifiable (n = 7). Finally, a total of 175 patients were enrolled in the study. Figure 1 shows the patient selection process.

Magnetic resonance imaging protocol

MRI exams were performed using a Philips 3 Tesla scanner (Philips Intera, release 10.3; Philips Medical Systems Nederland B.V., Best, the Netherlands) and a General Electric 1.5 Tesla scanner (Signa Horizon EchoSpeed, version 5.8; General Electric Healthcare, Milwaukee, WI, USA). All patients received a routine scan and an enhanced scan. Foam pads were placed in the lower abdomen to reduce breathing and motion artifacts.

The T2-weighted turbo spin-echo sequence was used in the transverse plane with the following parameters in the Shanxi Cancer Hospital: repetition time (RT): 3,590 ms; time to echo (TE): 120 ms; matrix: 432 × 432 mm; slice thickness: 4 mm; pixel spacing: 0.46 mm × 0.46 mm; series number: 602; and pixel bandwidth: 74 Hz/pixel. In The Second Affiliated Hospital of Army Medical University, the parameters were: RT: 4,000 ms; TE: 103 ms; matrix: 512 × 512 mm; slice thickness: 4 mm; pixel spacing: 0.50 mm × 0.50 mm; series number: 7; and pixel bandwidth, 122 Hz/pixel.

The parameters of the diffusion-weighted imaging (DWI) in the Shanxi Cancer Hospital were as follows: RT: 2,750 ms; TE: 50 ms; matrix: 256 × 256 mm; slice thickness: 5 mm; pixel spacing: 1.46 mm × 1.46 mm; series number: 901; and pixel bandwidth: 3,641 Hz/pixel. In The Second Affiliated Hospital of Army Medical University, the parameters were: RT: 5,600 ms; TE: 65 ms; matrix: 256 ×

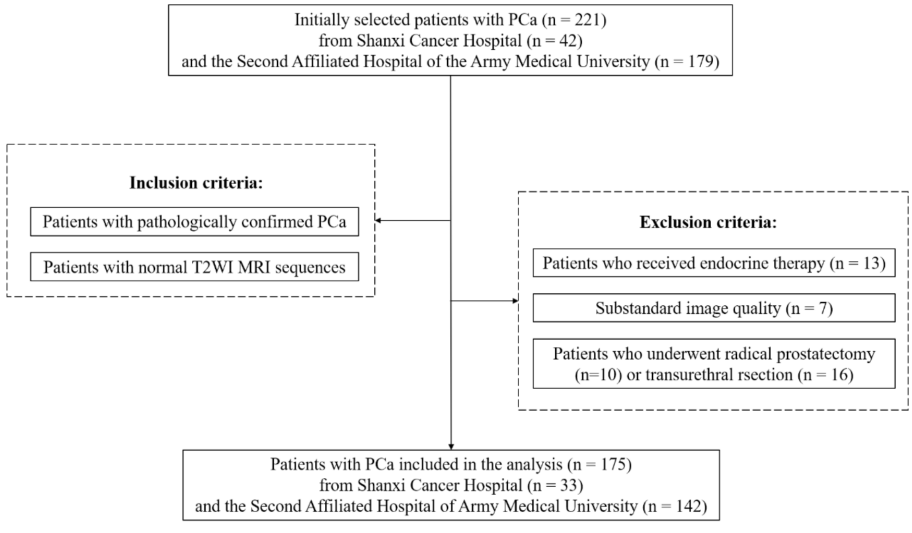

Figure 1. Flowchart of patient inclusion and exclusion. PCa, prostate cancer; T2WI, T2-weighted imaging; MRI, magnetic resonance imaging.

256 mm; slice thickness: 4 mm; pixel spacing: 1.56 mm × 1.56 mm; series number: 7; and pixel bandwidth: 1.953 Hz/pixel.

Clinical information

The authors collected clinical information on each patient from their medical records, including age, body mass index (BMI), free-PSA and total-PSA (f-PSA/t-PSA) levels, pathological T-stage, SV invasion or not, invasion of the surrounding structures, such as the bladder, rectum, or neurovascular bundles (NVB), and the tumor location.

Image pre-processing and segmentation

The patients were divided into four groups based on their pathological T-stage (T1–T4). To obtain a PCa 3D reconstruction model for further analysis, the authors uploaded the MRI images in Digital Imaging and Communications in Medicine (DICOM) format from the workstation to Amira software (Vision 2019, Thermo Fisher Scientific Inc., Waltham, MA, USA). The window level and window width were adjusted to optimize the visualization of the prostate zones. The segmentation of each MRI image in this study was performed by a junior urological surgeon with 3 years of working experience, and the segmentation result was further reviewed and corrected, if necessary, by a senior radiologist with 14 years of working experience, with the modified results being used for the morphological parameter calculations. The segmentation process was based on the division theory of prostate anatomical zones proposed by McNeal[2], and the recording of the tumor location refers to the sequences of apparent diffusion coefficient and DWI (b = 1000 s/mm^2) (Figure 2).

Three-dimensional prostate cancer reconstruction

After image segmentation, the 3D PCa models were reconstructed through the Generate Surface module of the Amira software. In this software, the models can move, scale, and rotate in all directions.

Data measurement based on the two-dimensional plane and three-dimensional prostate cancer reconstruction

According to the guidelines of the European Society of Urogenital Radiology, all images in the two-dimensional (2D) plane were retrospectively analyzed by a senior radiologist (with 14 years of working experience) who was unaware of the pathological results and all the clinical information.[13] The staging of the mpMRI was performed using the extracapsular extension (ECE) score introduced by Mehralivand et al.[14] The ECE score criteria were as follows: (a) grade 0, no suspicion of pathological ECE; (b) grade 1, either a curved contact length ≥1.5 cm or an irregular capsule or bulge; (c) grade 2, both of the above in grade 1; and (d) grade 3, obvious envelope breakthrough. The tumor's major axis (TA) was the maximal value of the tumor's diameter in three-axis planes using a MicroDICOM viewer (Solvusoft Corporation, Las Vegas, NV, USA).

In the 3D PCa reconstruction model, the PV, PZ volume (PZV), TZ volume (TZV), CZ volume (CZV), AFMS volume (AFMSV), and TV were measured using the surface area volume module in the Amira software. These were then used to analyze the relationship between the volume and T-stage. After that, the PZV/PV, TZV/PV, CZV/PV, and AFMSV/PV ratios were obtained by individually dividing PZV, TZV, CZV, and AFMSV by PV.

Statistical analysis

All statistical analyses were performed using the Statistical Package for the Social Sciences Statistics, version 25.0 (IBM Corp., Armonk, NY, USA). The number of PCa lesions was expressed as frequencies (percentages). Categorical data were analyzed using Pearson's chi-squared test and continuous data with the One-Way analysis of variance and independent samples t-test. Spearman's rank correlation coefficient was used to analyze the relationship between the multivariate parameters and the T-stage. All *P* values were two-sided, and those $P < 0.050$ were considered statistically significant.[15]

The receiver operating characteristic (ROC) curves analysis was used to determine the cut-off values of the different T-stages and evaluate the predictive performance of the morphological parameters for the T-stage diagnosis. The performance characteristics, including the area under the curve (AUC) of the ROC curve, sensitivity, and specificity, were also analyzed. The optimal cut-off values were calculated according to the formula (Youden's J index = sensitivity + specificity - 1), which is meaningful when its AUC >0.6.[16,17]

Results

Baseline characteristics

In this study, the authors enrolled 175 patients with PCa treated at the Shanxi Cancer Hospital (n = 40) and The Second Affiliated Hospital of Army Medical University (n = 135). According to the eighth edition of the American Joint Committee on Cancer staging criteria, the patients were divided into T1 (n = 25), T2 (n = 80), T3 (n = 36), and T4 (n = 34) stages. Age and BMI did not differ among the T-stage groups ($P = 0.261$ and $P = 0.315$), but the f-PSA/t-PSA levels significantly decreased from T1 to T4 ($P < 0.001$), 51.43% of patients (126/175) had a Gleason score (GS) of 4 + 4 or greater ($P < 0.001$), and the ECE score increased in accordance with the pathological T-stage ($P < 0.001$) (Table 1).

Tumor location

Table 2 presents the tumor locations based on the T-stage. In all patients, most tumors were in the PZ (45.7%), followed by the PZ and TZ (33.7%), then the TZ (7.6%). No tumors were in the CZ or AFMS. Approximately 24.0% of T1 and 10.0% of T2 tumors were difficult to identify on MRI. Furthermore, 58.3% (21/36) of T3 and 76.5% (26/34) of T4 tumors had invaded the SV. Approximately 50.0% (17/34) of T4 tumors had invaded the urethra, bladder, rectum, NVB, or other surrounding structures. Figure 3 illustrates the tumor changes in randomly selected, representative cases from each T-stage; these images show how the tumor area gradually increased from T1 to T4, indicating an overall increase in tumor aggressiveness.

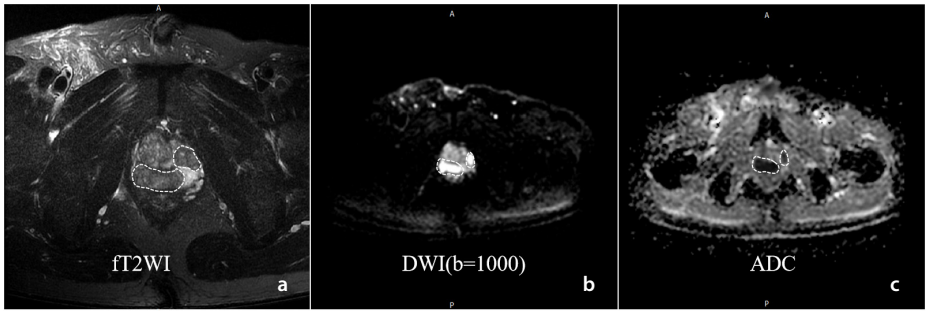

Figure 2. Tumor segmentation (dashed box) on different magnetic resonance imaging sequences, including T2WI **(a)**, DWI (b = 1000 s/mm^2) **(b)**, and ADC map **(c)** (Software: Syngo Quick Brower). fT2WI, fat-suppressed T2 weighted imaging; DWI, diffusion-weighted imaging; ADC, apparent diffusion coefficient.

Table 1. Demographic information of patients with prostate cancer at different tumor stages

	T1 (n = 25)	T2 (n = 80)	T3 (n = 36)	T4 (n = 34)	*P*	Total
Age (y)	73.88 ± 9.50	70.61 ± 10.53	71.47 ± 7.98	71.48 ± 9.16	0.261[a]	71.67 ± 8.88
BMI (kg/m^2)	21.86 ± 3.26	24.63 ± 3.44	23.48 ± 3.09	23.28 ± 2.95	0.315[a]	22.15 ± 3.53
f-PSA/t-PSA (ng/mL)	0.20 ± 0.07	0.18 ± 0.12	0.15 ± 0.10	0.11 ± 0.08	0.000[a]	0.16 ± 0.13
MRI-based ECE score					0.000[b]	
0	25/25(100.00%)	74/80 (92.50%)	0/36 (0.00%)	0/34 (0.00%)	-	99/175 (56.57%)
1	0/25 (0.00%)	6/80 (7.50%)	7/36 (19.44%)	0/34 (0.00%)	-	13/175 (7.43%)
2	0/25 (0.00%)	0/80 (0.00%)	29/36 (80.56%)	6/34 (17.65%)	-	35/175 (20.00%)
3	0/25 (0.00%)	0/80 (0.00%)	0/36 (0.00%)	28/34 (100.00%)	-	28/175 (16.00%)
Biopsy GS					0.000[b]	
GS = 3 + 3	13/25 (52.94%)	9/80 (11.25%)	1/36 (2.12%)	0/34 (0.00%)	-	23/175 (13.14%)
GS = 3 + 4	12/25 (47.06%)	14/80 (17.50%)	5/36 (14.89%)	0/34 (0.00%)	-	31/175 (17.71%)
GS = 4 + 3	0/25 (0.00%)	17/80 (21.25%)	8/36 (21.27%)	6/34 (17.39%)	-	31/175 (17.71%)
GS ≥ 4 + 4	0/25 (0.00%)	40/80 (50.00%)	22/36 (61.70%)	28/34 (82.61%)	-	90/175 (51.43%)

Unless indicated otherwise, the data specifies the number of cases, with percentages in parentheses. [a], One-Way analysis of variance; [b], Pearson's chi-squared test. T, tumor; BMI, body mass index; PSA, prostate-specific antigen; f-PSA/t-PSA, free-PSA/total-PSA; MRI, magnetic resonance imaging; ECE, extracapsular extension; GS, Gleason score.

Table 2. Tumor distributions of patients with prostate cancer at different tumor stages

Distribution of cancer foci (number of patients, ratio)	T-stage of PCa				Total
	T1 (n = 25)	T2 (n = 80)	T3 (n = 36)	T4 (n = 34)	
Tumors located only in the PZ	16 (64.0%)	43 (53.8%)	12 (33.3%)	10 (26.5%)	81 (46.3%)
Tumors located only in the TZ	2 (8.0%)	7 (8.7%)	4 (11.1%)	0 (0.0%)	13 (7.4%)
Tumors located in the PZ and TZ	1 (4.0%)	22 (27.5%)	20 (55.6%)	24 (67.6%)	67 (38.3%)
Tumors invading the SV	0 (0.0%)	0 (0.0%)	21 (58.3%)	26 (76.5%)	47 (26.9%)
Tumors invading adjacent structures	0 (0.0%)	0 (0.0%)	0 (0.0%)	17 (50.0%)	17 (9.7%)
Tumors that are difficult to identify	6 (24.0%)	8 (10.0%)	0 (0.0%)	0 (0.0%)	14 (8.0%)

The data specifies the number of cases, with percentages in parentheses. T, tumor; PCa, prostate cancer; PZ, peripheral zone; TZ, transition zone; SV, seminal vesicles.

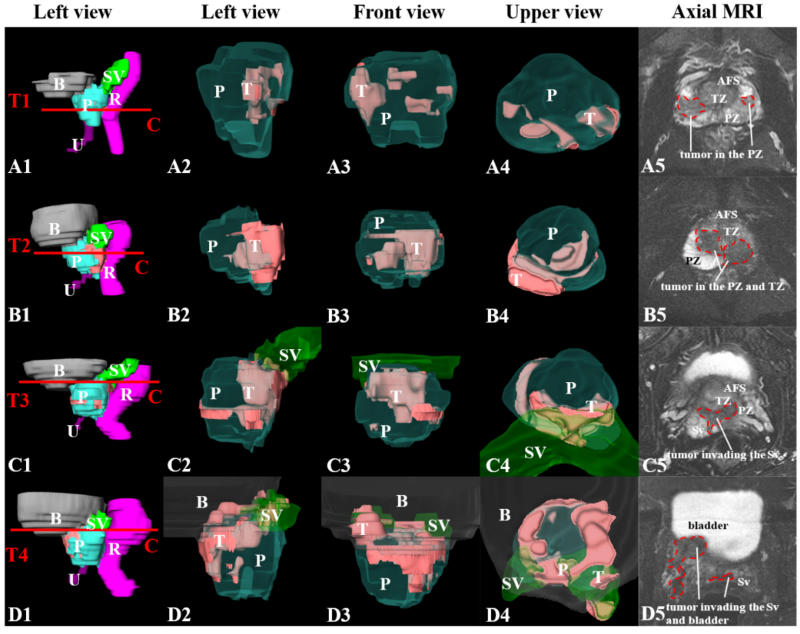

Figure 3. Three-dimensional reconstruction, spatial relationship, and location of prostate cancer lesions in different T-stages. **Column A1–D1**, three-dimensional reconstruction of the prostate and adjacent structures in the left view. **Column A2–D2, A3–D3, and A4–D4**, three-dimensional reconstruction of the tumor and prostate in the left, front, and upper views, in which the prostate, seminal vesicles, and bladder are semi-transparent. **Column A5–D5**, tumor segmentation in axial magnetic resonance images. **Row A1–A5**, T1 PCa; row **B1–B5**: T2 PCa; **row C1–C5**, T3 PCa; **row D1–D5**, T4 PCa. PCa, prostate cancer; PZ, peripheral zone; TZ, transition zone; CZ, central zone; AFMS, anterior fibromuscular stroma; B, bladder; SV, seminal vesicles; R, rectum; U, urethral canal; P, prostate; T-stages, tumor-stages.

Measurement and comparison of different tumor-stage three-dimensional models of prostate cancer

The PV, PZV, CZV, TA, TV, and TV/PV significantly differed as the T-stage increased (Table 3). The mean PZV value initially decreased and then increased from T1 to T4 ($P = 0.001$), and T2 was the inflection point. The mean PV and CZV values continuously decreased from T1 to T4 (r_s: -0.213, $P = 0.005$ and r_s: -0.288, $P = 0.006$). The TZV, AFMSV, PZV/TZV, PZV/PV, TZV/PV, CZV/PV, and AFMSV/PV did not differ based on the T-stage. Figure 4 demonstrates the prostatic zone changes in a randomly selected, representative case from each T-stage. The mean TA, TV, and TV/PV values significantly and continuously increased from T1 to T4 ($P < 0.050$) (Table 3).

The PV, PZV, CZV, TA, TV, and TV/PV significantly differed in the T1 to T2 group ($P = 0.001$, $P < 0.001$, $P = 0.021$, $P = 0.008$, $P = 0.003$, and $P < 0.001$, respectively). Furthermore, the TA, TV, and TV/PV significantly differed in the T2 to T3 group ($P < 0.001$, $P = 0.020$, and $P = 0.005$, respectively). Finally, the TA, TV, and TV/PV significantly differed in the T3 to T4 group ($P = 0.004$, $P = 0.010$, and $P = 0.008$, respectively) (Table 4).

Receiver operating characteristic curve analysis

A ROC curve analysis was used to predict the performance of the morphological

Table 3. Morphological parameter comparisons among the tumor stages of prostate cancer

	T-stage of PCa					Total (n = 175)
	T1 (n = 25)	T2 (n = 80)	T3 (n = 36)	T4 (n = 34)	*P*	
PV (cm)	**47.83 ± 18.80**	**38.39 ± 21.64**	**36.35 ± 28.72**	**34.17 ± 15.87**	**0.040**	**37.41 ± 20.95**
PZV (cm)	**17.42 ± 9.77**	**11.47 ± 5.22**	**11.57 ± 10.02**	**12.95 ± 7.29**	**0.003**	**12.33 ± 7.56**
TZV (cm)	25.76 ± 14.39	18.41 ± 13.36	22.97 ± 22.14	22.43 ± 18.67	0.204	21.18 ± 16.83
CZV (cm)	**2.28 ± 1.60**	**1.76 ± 1.53**	**1.50 ± 1.49**	**0.94 ± 1.24**	**0.006**	**1.62 ± 1.54**
AFMSV (cm)	2.38 ± 1.13	2.53 ± 1.74	2.16 ± 1.73	1.81 ± 1.20	0.153	2.29 ± 1.59
PZV/TZV	0.89 ± 0.47	1.22 ± 2.11	0.77 ± 0.60	0.64 ± 0.60	0.219	0.28 ± 0.14
PZV/PV	0.38 ± 0.12	0.36 ± 0.17	0.35 ± 0.18	0.36 ± 0.19	0.992	0.36 ± 0.17
TZV/PV	0.50 ± 0.14	0.49 ± 0.17	0.53 ± 0.19	0.52 ± 0.23	0.732	0.51 ± 0.18
CZV/PV	0.05 ± 0.04	0.05 ± 0.04	0.05 ± 0.05	0.04 ± 0.05	0.357	0.05 ± 0.05
AFMSV/PV	0.05 ± 0.03	0.07 ± 0.04	0.05 ± 0.04	0.07 ± 0.08	0.115	0.07 ± 0.05
TA (mm)	**1.55 ± 0.84**	**2.23 ± 1.13**	**3.39 ± 1.25**	**4.45 ± 1.67**	**0.000**	**2.80 ± 1.59**
TV (cm)	**1.91 ± 2.68**	**7.10 ± 14.13**	**15.52 ± 18.5**	**29.93 ± 25.14**	**0.000**	**12.52 ± 19.45**
TV/PV	**0.04 ± 0.04**	**0.14 ± 0.16**	**0.25 ± 0.24**	**0.42 ± 0.20**	**0.000**	**0.20 ± 0.21**

Bold are the results of good predictive performance. *P*, One-Way analysis of variance. T, tumor; PV, prostate volume; PZV, peripheral zone volume; TZV, transition zone volume; CZV, central zone volume; AFMSV, anterior fibromuscular stroma volume; PZV/TZV, the ratio of PZV and TZV; PZV/PV, the ratio of PZV and PV; TZV/PV, the ratio of TZV and PV; CZV/PV, the ratio of CZV and PV; AFMSV/PV, the ratio of AFMSZV and PV; TA, tumor's major axis; TV, tumor volume; TV/PV, the ratio of TV and PV.

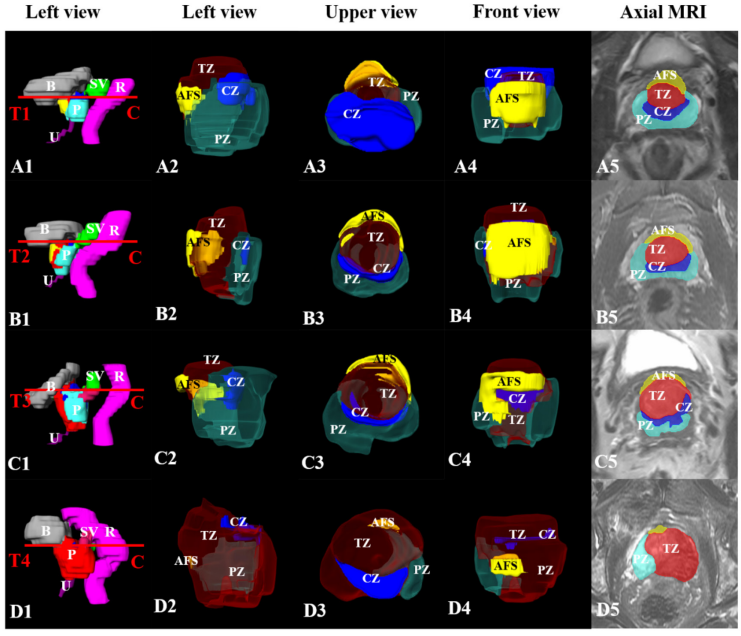

Figure 4. Anatomic morphology, three-dimensional shape, and spatial relationship of prostatic zones in different tumor stages. **Column A1–D1**, three-dimensional reconstruction of the prostate and adjacent structures in the left view. **Column A2–D2, A3–D3, and A4–D4**, three-dimensional reconstruction of the PZ, TZ, CZ, and AFMS in the left, upper, and front view, in which the PZ and TZ are semi-transparent. **Column A5–D5**, PZ, TZ, CZ, and AFMS segmentation in axial magnetic resonance imaging. **Row A1–A5**, T1 PCa; **row B1–B5**, T2 PCa; **row C1–C5**, T3 PCa; **row D1–D5**, T4 PCa. PCa, prostate cancer; PZ, peripheral zone; TZ, transition zone; CZ, central zone; AFMS, anterior fibromuscular stroma; B, bladder; SV, seminal vesicle; R, rectum; U, urethral canal; P, prostate.

parameters in the T-stage diagnosis (Figure 5). Table 5 summarizes the performance characteristics, such as the AUC, sensitivity, and specificity. The cut-off values of the PV, PZV, CZV, TA, TV, and the ratio of TV/PV for discrimination of T1 and T2 were 53.63 cm^3, 11.60 cm^3, 1.97 cm^3, 2.30 mm, 0.90 cm^3, and 0.03 (AUCs: 0.628, 0.658, 0.610, 0.689, 0.724, and 0.764), respectively. The cut-off values of the TA, TV, and the ratio of TV/PV for discrimination of T2 and T3 were 2.80 mm, 8.29 cm^3, and 0.12 (AUCs: 0.769, 0.702, and 0.688), respectively. The cut-off values of the TA, TV, and the ratio of TV/PV for discrimination of T3 and T4 were 4.17 mm, 18.71 cm^3, and 0.22 (AUCs: 0.674, 0.709, and 0.729), respectively.

Discussion

ECE (stage T3a or more) is associated with a higher risk of positive surgical margins, biochemical recurrence (BCR), and metastasis, and a lower cancer-specific survival rate.[18] Accurate detection of ECE is essential to maintaining urinary continence and sexual ability.[19] Therefore, it is necessary to diagnose the PCa T-stage before surgery correctly. In this study, the authors retrospectively analyzed the relationships between the morphological parameters and PCa T-stage based on 3D reconstructions after manually segmenting the MRI images. The study's results showed that the morphology of the prostate zones and tumors could predict the PCa T-stage.

Previous authors have pointed out that 3D-based scores better define the complexity of tumors and have higher predictive accuracy for postoperative complications than 2D-based ones.[20] However, the potential applications of 3D reconstruction are yet to be fully studied, and the information that can be extracted from 3D virtual models and their refinement has yet to be explored. The authors have identified new morphological and volumetric parameters from the 3D model.

In this study, 46.3% of tumors were only in the PZ. In contrast, 7.4% of tumors were only in the TZ. Yang et al.[21] also reported many more tumors in the PZ than in the TZ, with a high-grade GS of 8 and 9 (38.5% vs. 24.3%). Additionally, Ali et al.[22] suggested that PCa in the TZ had better clinical outcomes than PCa in the PZ and CZ. Similarly, Sato et al.[23] indicated that conservative treatment could be used for PCa in the TZ and that these patients had a better prognosis than those with PCa in the PZ and CZ. The authors hypothesize that this may be related to increased androgen dependency within the PZ, leading to the occurrence and development of PCa in the PZ.[24]

This study found that the PV gradually decreased from stage T1 to T4 ($P < 0.050$), consistent with studies that found that the

Table 4. Morphological parameter comparisons among the consequent tumor stages of prostate cancer

	T1 (n = 25)	T2 (n = 80)	*P*	T2 (n =8 0)	T3 (n = 36)	*P*	T3 (n = 36)	T4 (n = 34)	*P*
PV (cm^3)	**47.83 ± 18.80**	**38.39 ± 21.64**	**0.001**	38.39 ± 21.64	36.35 ± 28.72	0.317	53.87 ± 34.06	68.04 ± 38.56	0.749
PZV (cm^3)	**17.42 ± 9.77**	**11.47 ± 5.22**	**0.000**	11.47 ± 5.22	11.57 ± 10.02	0.864	11.57 ± 10.02	12.95 ± 7.29	0.808
TZV (cm^3)	25.76 ± 14.39	18.41 ± 13.36	0.167	18.41 ± 13.36	22.97 ± 22.14	0.173	22.97 ± 22.14	22.43 ± 18.67	0.913
CZV (cm^3)	**2.28 ± 1.60**	**1.76 ± 1.53**	**0.121**	1.76 ± 1.53	1.50 ± 1.49	0.4	1.50 ± 1.49	0.94 ± 1.24	0.097
AFMSV (cm^3)	2.38 ± 1.13	2.53 ± 1.74	0.688	2.53 ± 1.74	2.16 ± 1.73	0.294	2.16 ± 1.73	1.81 ± 1.20	0.329
PZV/TZV	0.89 ± 0.47	1.22 ± 2.11	0.44	1.22 ± 2.11	0.77 ± 0.60	0.222	0.77 ± 0.60	0.64 ± 0.60	0.398
PZV/PV	0.38 ± 0.12	0.36 ± 0.17	0.623	0.36 ± 0.17	0.35 ± 0.18	0.745	0.24 ± 0.12	0.18 ± 0.10	0.93
TZV/PV	0.50 ± 0.14	0.49 ± 0.17	0.855	0.49 ± 0.17	0.53 ± 0.19	0.312	0.41 ± 0.18	0.32 ± 0.16	0.921
CZV/PV	0.05 ± 0.04	0.05 ± 0.04	0.833	0.05 ± 0.04	0.05 ± 0.05	0.647	0.03 ± 0.04	0.02 ± 0.03	0.292
AFMSV/PV	0.05 ± 0.03	0.07 ± 0.04	0.057	0.07 ± 0.04	0.05 ± 0.04	0.130	0.05 ± 0.03	0.03 ± 0.02	0.349
TA (mm)	**1.55 ± 0.84**	**2.23 ± 1.13**	**0.008**	**2.23 ± 1.13**	**3.39 ± 1.25**	**0.000**	**3.39 ± 1.25**	**4.45 ± 1.67**	**0.004**
TV (cm^3)	**1.91 ± 2.68**	**7.10 ± 14.13**	**0.003**	**7.10 ± 14.13**	**15.52 ± 18.5**	**0.020**	**15.52 ± 18.5**	**29.93 ± 25.14**	**0.010**
TV/PV	**47.83 ± 18.80**	**38.39 ± 21.64**	**0.000**	**38.39 ± 21.64**	**36.35 ± 28.72**	**0.005**	**0.25 ± 0.24**	**0.42 ± 0.20**	**0.008**

P, independent samples t-test. T, tumor; PV, prostate volume; PZV, peripheral zone volume; TZV, transition zone volume; CZV, central zone volume; AFMSV, anterior fibromuscular stroma volume; PZV/TZV, the ratio of PZV and TZV; PZV/PV, the ratio of PZV and PV; TZV/PV, the ratio of TZV and PV; CZV/PV, the ratio of CZV and PV; AFMSV/PV, the ratio of AFMSZV and PV; TA: tumor's major axis; TV, tumor volume; TV/PV, the ratio of TV and PV.

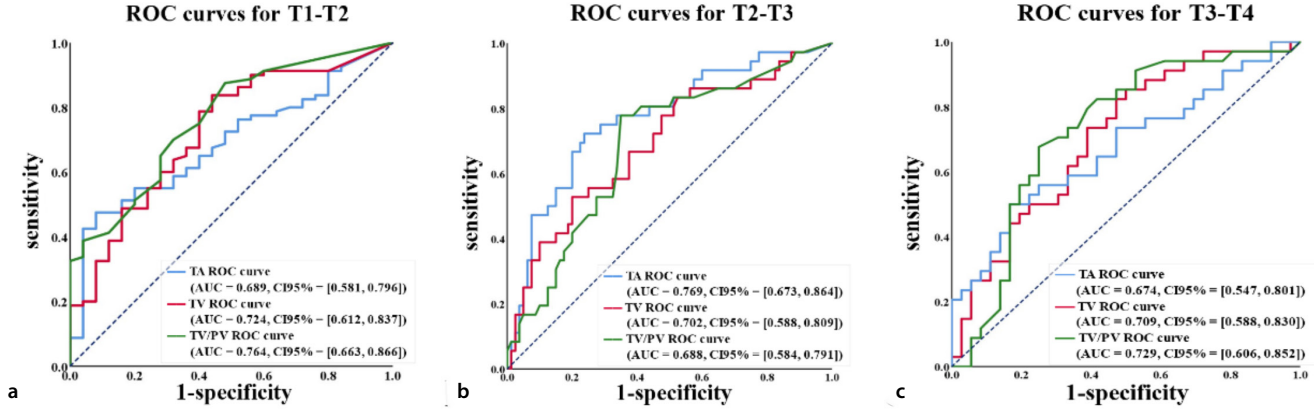

Figure 5. Receiver operating characteristic curves of the morphological parameters of the tumors for discrimination of T1 and T2 **(a)**, T2 and T3 **(b)**, and T3 and T4 **(c)**. TA, tumor's major axis; TV, tumor volume; TV/PV, the volume ratio of TV and PV; ROC, receiver operating characteristic; AUC, area under the curve.

Table 5. The cut-off values, area under the curve, sensitivity, and specificity for the differentiation of the tumor stages of prostate cancer

		Cut-off	AUC	Sensitivity	Specificity
T1–T2	PV (cm^3)	53.63	0.628 (0.469, 0.787)	0.579	0.789
	PZV (cm^3)	11.60	0.658 (0.530, 0.786)	0.895	0.404
	CZV (cm^3)	1.97	0.610 (0.445, 0.749)	0.599	0.764
	TA (mm)	2.30	0.689 (0.581, 0.796)	0.475	0.920
	TV (cm^3)	0.90	0.724 (0.612, 0.837)	0.838	0.560
	TV/PV	0.03	0.764 (0.663, 0.866)	0.901	0.620
T2–T3	TA (mm)	2.80	0.769 (0.673, 0.864)	0.778	0.762
	TV (cm^3)	8.29	0.702 (0.588, 0.809)	0.528	0.800
	TV/PV	0.12	0.688 (0.584, 0.791)	0.722	0.650
T3–T4	TA (mm)	4.17	0.674 (0.547, 0.801)	0.500	0.833
	TV (cm^3)	18.71	0.709 (0.588, 0.830)	0.676	0.500
	TV/PV	0.22	0.729 (0.606, 0.852)	0.853	0.750

T, tumor; PV, prostate volume; PZV, peripheral zone volume; CZV, central zone volume; TA, tumor's major axis; TV, tumor volume; TV/PV, the ratio of TV and PV; AUC, area under the curve.

PV negatively correlated with the incidence rate and aggressiveness of PCa.[25-27] Previous histo-anatomical studies showed that TZ growth leads to secondary atrophy and PZ tissue apoptosis and necrosis, which may explain why increased TZV inhibits PCa. However, the authors found no differences among the T-stages for TZV or the TZV/PZV ratio, perhaps due to an insufficient sample size.

The hypothesis that the TV is the most important PCa prognostic indicator remains controversial.[28] Some studies have reported a strong correlation between the TV and BCR, and the authors of these studies thought that the clinical failure (CF) rate of patients with PCa with a TV of less than 0.5 cc is low.[29,30] However, Mayer et al.[31] reported that histology-based TV is related to the GS (r = 0.498, P = 0.0098), and Baba et al.[9] suggested that the optimal TV cut-off value for predicting BCR was 2.8 cc (AUC: 0.690). Moreover, Castiglione et al.[32] concluded that for high-risk patients with PCa, a TV >6.29 cc (AUC: 0.722) leads to CF, and Dong et al.[33] reported that the optimal cut-off value for identifying the best maximum standardized uptake value (SUV_{max}) for high-risk patients with PCa was 9.61 (AUC: 0.828). Furthermore, Jiao et al.[34] established and prospectively verified that the optimal SUV_{max} cut-off value for discriminating clinically significant PCa from BPH was 5.30, with AUCs of 0.893 in the training and 0.853 in the prospective validation cohorts. However, no prior studies have analyzed the diagnostic value of the TA, TV, and TV/PV for the T-stage diagnoses of PCa.

Finally, the authors assessed the relationships between the tumor's morphological parameters and the T-stage. They found that the TA, TV, and TV/PV gradually increased from stage T1 to T4 (P < 0.050), which agreed with Yuk et al.'s[35] study. The authors also found that the higher the T-stage, the greater the cut-off value, indicating that the tumor's morphological parameters are important indicators for the T-stage diagnosis. Therefore, the authors considered that the TA, TV, and TV/PV can predict the T-stage in patients with PCa.

This study has four limitations. First, the study population only included the Asian population, whose PCa incidence rates, mortality rates, and PV are lower than those of Western populations. Therefore, more institutions should be involved in any future study. Second, the authors evaluated the correlations between the morphological parameters in MRI and the T-stage, ignoring the microscopic pathological changes. Thus, further genomics and pathological analysis are needed.[34] Third, manual segmentation is time-consuming and labor-intensive, resulting in a small sample size. In the future, artificial intelligence should be used to assist in segmentation to reduce the segmentation time. Fourth, there are some errors in manual segmentation due to fatigue and personal subjectivity. As a next step, the authors will invite more experts to verify the segmentation in this study.

In conclusion, the morphological parameters of the prostate zones and prostate tumor significantly differed among the T-stages, including the PV, PZ's volume, CZ's volumes, TA, TV, and the TV/PV ratio. Based on MRI 3D reconstruction, the TA, TV, and TV/PV are the key indicators of the PCa T-stage diagnosis, which can help to make accurate diagnoses and lateral treatment decisions.

Acknowledgements

The authors thank Editage (www.editage.cn) for English language editing.

Conflict of interest disclosure

The authors declared no conflicts of interest.

Funding

This study received funding from the National Natural Science Foundation of China (31971113), the Chongqing Science and Technology Talent project (CQYC201905037), the Army Science and Technology Talent project (91003201901973), and the Qingbo Project of The Second Affiliated Hospital of Army Medical University (2022YQB043).

References

1. Sung H, Ferlay J, Siegel RL, et al. Global Cancer Statistics 2020: GLOBOCAN estimates of incidence and mortality worldwide for 36 cancers in 185 countries. *CA Cancer J Clin*. 2021;71(3):209-249. [CrossRef]
2. McNeal JE. The zonal anatomy of the prostate. *Prostate*. 1981;2(1):35-49. [CrossRef]
3. Giganti F, Allen C. Imaging quality and prostate MR: it is time to improve. *Br J Radiol*. 2021;94(1118):20200934. [CrossRef]
4. Schoots IG, Roobol MJ, Nieboer D, Bangma CH, Steyerberg EW, Hunink MG. Magnetic resonance imaging-targeted biopsy may enhance the diagnostic accuracy of significant prostate cancer detection compared to standard transrectal ultrasound-guided biopsy: a systematic review and meta-analysis. *Eur Urol*. 2015;68(3):438-450. [CrossRef]
5. No authors listed. Hematuria in adults. *N Engl J Med*. 2021;385:576. [CrossRef]
6. Marenco J, Orczyk C, Collins T, Moore C, Emberton M. Role of MRI in planning radical prostatectomy: what is the added value? *World J Urol*. 2019;37:1289-1292. [CrossRef]
7. Colvin R, Walker D, Hafron J, et al. Which measurement method should be used for prostate volume for PI-RADS? A comparison of ellipsoid and segmentation methods. *Clin Imaging*. 2021;80:454-458. [CrossRef]
8. Hamzaoui D, Montagne S, Granger B, et al. Prostate volume prediction on MRI: tools, accuracy and variability. *Eur Radiol*. 2022;32:4931-4941. [CrossRef]
9. Baba, H, Sakamoto S, Zhao X, et al. Tumor location and a tumor volume over 2.8 cc predict the prognosis for Japanese localized prostate cancer. *Cancers (Basel)*. 2022;14(23):5823. [CrossRef]

10. Tan N, Lin WC, Khoshnoodi P, et al. In-Bore 3-T MR-guided transrectal targeted prostate biopsy: prostate imaging reporting and data system version 2-based diagnostic performance for detection of prostate cancer. *Radiology*. 2017;283(1):130-139. [CrossRef]
11. Hoeks CM, Hambrock T, Yakar D, et al. Transition zone prostate cancer: detection and localization with 3-T multiparametric MR imaging. *Radiology*. 2013;266(1):207-217. [CrossRef]
12. Liang W, Qiubai L, Alberto Hebert V. Prostate MRI anatomical partition. *China J Radiology*. 2020;54:1038-1040. [CrossRef]
13. Turkbey B, Rosenkrantz AB, Haider MA, et al. Prostate imaging reporting and data system version 2.1: 2019 update of prostate imaging reporting and data system version 2. *Eur Urol*. 2019;76:340-351. [CrossRef]
14. Mehralivand S, Shih JH, Harmon S, et al. A grading system for the assessment of risk of extraprostatic extension of prostate cancer at multiparametric MRI. *Radiology*. 2019;290:709-719. [CrossRef]
15. Obuchowski NA, Bullen JA. Receiver operating characteristic (ROC) curves: review of methods with applications in diagnostic medicine. *Phys Med Biol*. 2018;63(7):07TR01. [CrossRef]
16. Nahm FS. Receiver operating characteristic curve: overview and practical use for clinicians. *Korean J Anesthesiol*. 2022;75(1):25-36. [CrossRef]
17. Njor SH, Andersen B, Friis-Hansen L, et al. The optimal cut-off value in fit-based colorectal cancer screening: An observational study. *Cancer Med*. 2021;10(5):1872-1879. [CrossRef]
18. Chang AJ, Autio KA, Roach M 3rd, Scher HI. High-risk prostate cancer-classification and therapy. *Nat Rev Clin Oncol*. 2014;11(6):308-323. [CrossRef]
19. Sighinolfi MC, Assumma S, Cassani A, et al. Pre-operative prediction of extracapsular extension of prostate cancer: first external validation of the PRECE model on an independent dataset. *Int Urol Nephrol*. 2023;55(1):93-97. [CrossRef]
20. Bianchi L, Schiavina R, Bortolani B, et al. Novel volumetric and morphological parameters derived from three-dimensional virtual modeling to improve comprehension of tumor's anatomy in patients with renal cancer. *Eur Urol Focus*. 2022;8(5):1300-1308. [CrossRef]
21. Yang L, Li M, Zhang MN, Yao J, Song B. Association of prostate zonal volume with location and aggressiveness of clinically significant prostate cancer: a multiparametric MRI study according to PI-RADS version 2.1. *Eur J Radiol* 2022;150, 110268. [CrossRef]
22. Ali A, Du Feu A, Oliveira P, Choudhury A, Bristow RG, Baena E. Prostate zones and cancer: lost in transition? *Nat Rev Urol*. 2022;19(2):101-115. [CrossRef]
23. Sato S, Kimura T, Onuma H, Egawa S, Takahashi H. Transition zone prostate cancer is associated with better clinical outcomes than peripheral zone cancer. *BJUI Compass*. 2020;2(3):169-177. [CrossRef]
24. Cancer Genome Atlas Research Network. The molecular taxonomy of primary prostate cancer. *Cell*. 2015;163(4):1011-1025. [CrossRef]
25. Frost JM, Smith LA, Sharma P, de Riese WT. Possible clinical implications of peripheral zone changes depending on prostate size. *Int Urol Nephrol*. 2019;51(10):1721-1726. [CrossRef]
26. Sellers J, Wagstaff RG, Helo N, de Riese WTW. Quantitative measurements of prostatic zones by MRI and their dependence on prostate size: possible clinical implications in prostate cancer. *Ther Adv Urol*. 2021;13:17562872211000852. [CrossRef]
27. Yamashiro JR, de Riese WTW. Any correlation between prostate volume and incidence of prostate cancer: a review of reported data for the last thirty years. *Res Rep Urol*. 2021;13:749-757. [CrossRef]
28. Wolters T, Roobol MJ, van Leeuwen PJ, et al. A critical analysis of the tumor volume threshold for clinically insignificant prostate cancer using a data set of a randomized screening trial. *J Urol*. 2011;185(1):121-125. [CrossRef]
29. Hashimoto Y, Okamoto A, Imai A, et al. Biochemical outcome of small-volume or insignificant prostate cancer treated with radical prostatectomy in Japanese population. *Int J Clin Oncol*. 2012;17(2):119-123. [CrossRef]
30. Reinhardt D, Helfand BT, Cooper PR, Roehl KA, Catalona WJ, Loeb S. Prostate cancer risk alleles are associated with prostate cancer volume and prostate size. *J Urol*. 2014;191(6):1733-1736. [CrossRef]
31. Mayer R, Simone CB, Turkbey B, Choyke P. Prostate tumor eccentricity predicts Gleason score better than prostate tumor volume. *Quant Imaging Med Surg*. 2022;12(2):1096-1108. [CrossRef]
32. Castiglione F, Dell'Oglio P, Tosco L, et al. Tumor volume and clinical failure in high-risk prostate cancer patients treated with radical prostatectomy. *Prostate*. 2017;77(1):3-9. [CrossRef]
33. Dong S, Li Y, Chen J, Li Y, Yang P, Li J. 18F-PSMA-1007 PET/CT-derived semi-quantitative parameters for risk stratification of newly diagnosed prostate cancer. *Front Oncol*. 2022;12:1025930. [CrossRef]
34. Jiao J, Kang F, Zhang J, et al. Establishment and prospective validation of an SUV (max) cutoff value to discriminate clinically significant prostate cancer from benign prostate diseases in patients with suspected prostate cancer by 68Ga-PSMA PET/CT: a real-world study. *Theranostics*. 2021;11(17):8396-8411. [CrossRef]
35. Yuk HD, Byun SS, Hong SK, Lee H. The tumor volume after radical prostatectomy and its clinical impact on the prognosis of patients with localized prostate cancer. *Sci Rep*. 2022;12(1):6003. [CrossRef]